

Numerical simulation of saline water intrusion in the Karnafuli river

LIAQAT ALI KHAN*

Department of Water Resources Engineering, Bangladesh University of Engineering and Technology, Dhaka, Bangladesh.

Received on August 17, 1987; Revised on May 23, 1988.

Abstract

A one-dimensional numerical model for the simulation of salinity intrusion in the Karnafuli river system, consisting of three branches connected at a junction, has been developed. The model was calibrated and validated by simulating salinity intrusion lengths under two widely different hydraulic conditions. The model calibration was also checked by comparing high- and low-water slack salinity data along the lower reach of the river. Assumption made in formulating sea-face boundary condition has been validated.

Key words: Salinity intrusion, numerical simulation, Karnafuli river, hydraulic conditions.

1. Introduction

The Karnafuli river rises in the Lushai Hills in India and follows a south-western course through the Chittagong Hill tracts and alluvial coastal plain in the south-eastern part of Bangladesh. Downstream of Chittagong it falls into the Bay of Bengal at Patenga. The Halda is the main tributary. The combined river system downstream of Kaptai dam is shown in fig. 1. At Patenga the river is subjected to strong tidal action. Fresh water inflow to the Karnafuli is controlled by the Kaptai dam, situated about 80 km from Patenga. The Halda is a flashy river with practically negligible inflow during the dry season.

Saline water from the Bay of Bengal pollutes the lower reach of the Karnafuli river. The extent of saline-water intrusion depends on the fresh water released from the Kaptai dam, the tide in the Bay of Bengal, the density difference between the river and sea waters and the geometry of the river. Dredging of the river for navigation by the Chittagong Port Authority (CPA) and upstream abstraction of water for irrigation produce changes in the salinity distribution in the river. To study the effects of dredging, upstream abstraction of water and other river training projects it is essential to develop a mathematical model. In the present study, a numerical model of the Karnafuli river system describing the movement of saline water has been developed. Many such models

* Present address: 83, Bosworth Street, Old Town, ME 04468, USA.

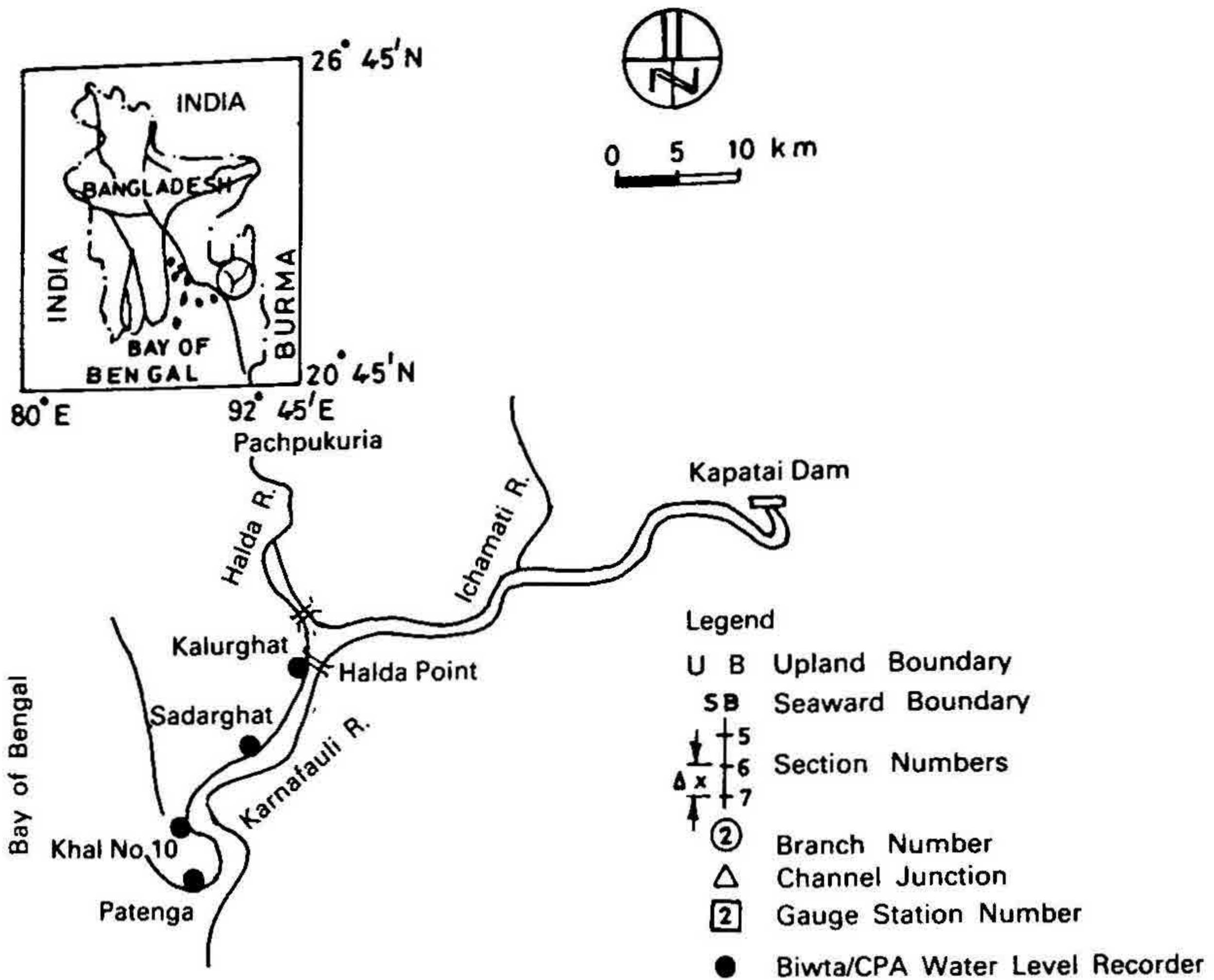


FIG. 1. Location map of the Karnafuli river.

have been proposed for estuarial networks^{1,2} in recent years. However, these are not generally available for local use. In Bangladesh, Khan and Alam³ and Chowdhury⁴ have developed simplified models which, however, cannot be applied to estuarial networks. This paper, therefore, briefly describes the model developed in this study and its application to the Karnafuli river.

2. Governing equations

Mathematically the problem of salinity intrusion in an estuarial network can be defined by three equations, namely, the continuity and momentum equations for flow of water and mass transport equation for salt. For one-dimensional flow these equations are

$$\frac{\partial H}{\partial t} + \frac{1}{B} \frac{\partial Q}{\partial x} = q \quad (1)$$

$$\frac{\partial Q}{\partial t} + \frac{2Q}{A} \frac{\partial Q}{\partial x} - \frac{Q^2}{A^2} \frac{\partial A}{\partial x} + gA \frac{\partial H}{\partial x} + gn^2 \frac{Q|Q|}{AR^{4/3}} = 0 \quad (2)$$

$$\frac{\partial}{\partial t}(AS) + \frac{\partial}{\partial x}(QS) = \frac{\partial}{\partial x} \left(AE \frac{\partial S}{\partial x} \right) \quad (3)$$

where

H = water surface elevation,	n = Manning's-roughness coefficient,
Q = flow rate,	g = gravitational acceleration,
q = lateral inflow per unit length of river,	S = salt-water concentration,
B = water surface width of channel,	E = longitudinal-dispersion coefficient,
A = cross-sectional area,	x = distance along channel axis, and
R = hydraulic radius,	t = time.

In equation (2) the effect of density difference between saline and fresh water has been neglected. This is a reasonable assumption for well-mixed estuaries⁵. The longitudinal-dispersion coefficient⁶ applicable to both fresh-and saline-water regions in an estuary is given by:

$$E(x, t) = K_1 \left| \frac{\partial S'}{\partial x'} \right| + K_2 nuR^{5/6} \quad (4)$$

where

$S' = S - S_o$,	K_1 = coefficient representing the degree of stratification in the estuary, and
S_o = salt concentration of sea water,	
$x' = x/L$,	K_2 = coefficient applicable to fresh-water region of estuary.
u = velocity of flow,	

Simultaneous solution of equations (1) and (2) provides the hydraulic information necessary for the solution of equation (3), which is also known as salt-balance equation.

3. Boundary conditions

For the solution of equations (1) and (2) external boundary conditions used are tidal stage hydrograph at Patenga and fresh-water inflows at Kaptai and Pachpukuria. Internal boundary conditions necessary at the confluence of the two rivers, representing a three-way junction are as follows:

$$A_p \frac{dH}{dt} + \sum_{i=1}^3 Q_i = 0 \quad (5)$$

$$H_1 = H_2 = H_3 \quad (6)$$

where A_p is the plan area of junction, and Q_i , discharge from the i th branch.

For equation (3), the only information necessary is the concentration of saline water in the Bay of Bengal near Patenga. During flood flow, salinity at Patenga is set equal to S_o . However, during ebb flow, boundary salinity values are computed by balancing total (advective + dispersive) salt flux across the boundary. The computation of sea-face boundary salinity, over the tidal cycle, is based on the concept of Thatcher and Harleman⁶. Upstream boundaries are outside the salinity-intrusion limit, where salinity is

always zero. The salt-continuity equation⁷ applicable to the junction of three channels is as follows:

$$\frac{\partial}{\partial t}(VS) + \sum_{i=1}^3 \left[QS - AE \frac{\partial S}{\partial x} \right] = 0 \quad (7)$$

where V is the volume of salt-water mixture contained in the junction.

4. Initial conditions

To start the computations, water surface is assumed horizontal and discharge zero throughout the river system. Salinity is assumed to vary linearly from S_0 at Patenga to zero at the confluence, the assumed limit of salinity intrusion in the Karnafuli river. Computations are repeated until quasi-steady conditions are reached.

5. Numerical model

The numerical model developed in this study neglects the effect of density difference between the sea water and the fresh water. Under this assumption, the solution of equations (1) and (2) can be decoupled from equation (3). The model, therefore, solves the dynamic equations and the salt-transport equation sequentially for each tidal cycle.

5.1 Hydrodynamic model

In this study, equations (1) and (2) were solved by Preissmann four-point implicit scheme⁸, and can be discretized to the following pair of algebraic equations:

$$a_i(H_i^{m+1}, H_{i+1}^{m+1}, Q_i^{m+1}, Q_{i+1}^{m+1}) = 0 \quad (8)$$

$$b_i(H_i^{m+1}, H_{i+1}^{m+1}, Q_i^{m+1}, Q_{i+1}^{m+1}) = 0. \quad (9)$$

In equations (8) and (9), m is time level and i represents section number in a river reach. The coefficients in these equations are functions of water levels and discharges at present time level and geometry of the river.

For a river system, equations (8) and (9) can be expressed as follows:

$$[C]\{Z\} = \{D\} \quad (10)$$

where $[C]$ is the coefficient matrix, $\{Z\}$ represents either water level or discharge and $\{D\}$ the column vector. In this study, the system of equation (10) was solved by double-sweep algorithm^{8,9} for tree-type river networks.

5.2 Salinity submodel

The salinity model computes S^{m+1} at the junction of channels explicitly, which is then used as internal boundary conditions for the connected branches. Salinity distribution in

the branches is then computed by an implicit formulation. Explicit solution of equation (7) can be expressed as follows⁷:

$$S^{m+1} = f(S^m). \tag{11}$$

To solve equation (3) for branches, Stone and Brian's¹⁰ six-point implicit scheme has been used. The application of this scheme results in the following equation for a computational cell:

$$c_i(S_{i-1}^{m+1}, S_i^{m+1}, S_{i+1}^{m+1}) = 0. \tag{12}$$

The coefficients of the equation are evaluated with tidal stage and discharge values obtained from the hydrodynamic model, the geometry of the river and salinity at the present time level. Writing equation (12) for each grid point in a given branch provides a system of equations which can be expressed in matrix notation by equation (10). In this case [C] is a tri-diagonal matrix and {Z} represents salinity at time $t = (m + 1)\Delta t$. Once boundary conditions are specified, this system of equation can again be solved by double-sweep algorithm^{3,8}. This process is then repeated for each branch in the network.

6. Schematization of the river

The Karnafuli-Halda river system consists of three branches, bounded by three external boundaries at Patenga, Kaptai and Pachpukuria and one internal boundary at Halda Point. The lower Karnafuli, from Patenga to Halda Point, has been discretized into smaller reaches of length 2.5 km. As the salinity intrusion in the other two reaches is not important, they were discretized with $\Delta x = 5$ km. The schematic representation of the river system is shown in fig. 2. The hydrodynamic model can compute water levels and discharges with variable grid spacing within the given branch. However, the use of Stone and Brian's scheme, correlating salinity at three consecutive grid points, restricts the use of such variable grid spacing for the simulation of salinity. The geometric properties at grid points were extracted⁹ from sounding charts obtained from the CPA; sounding

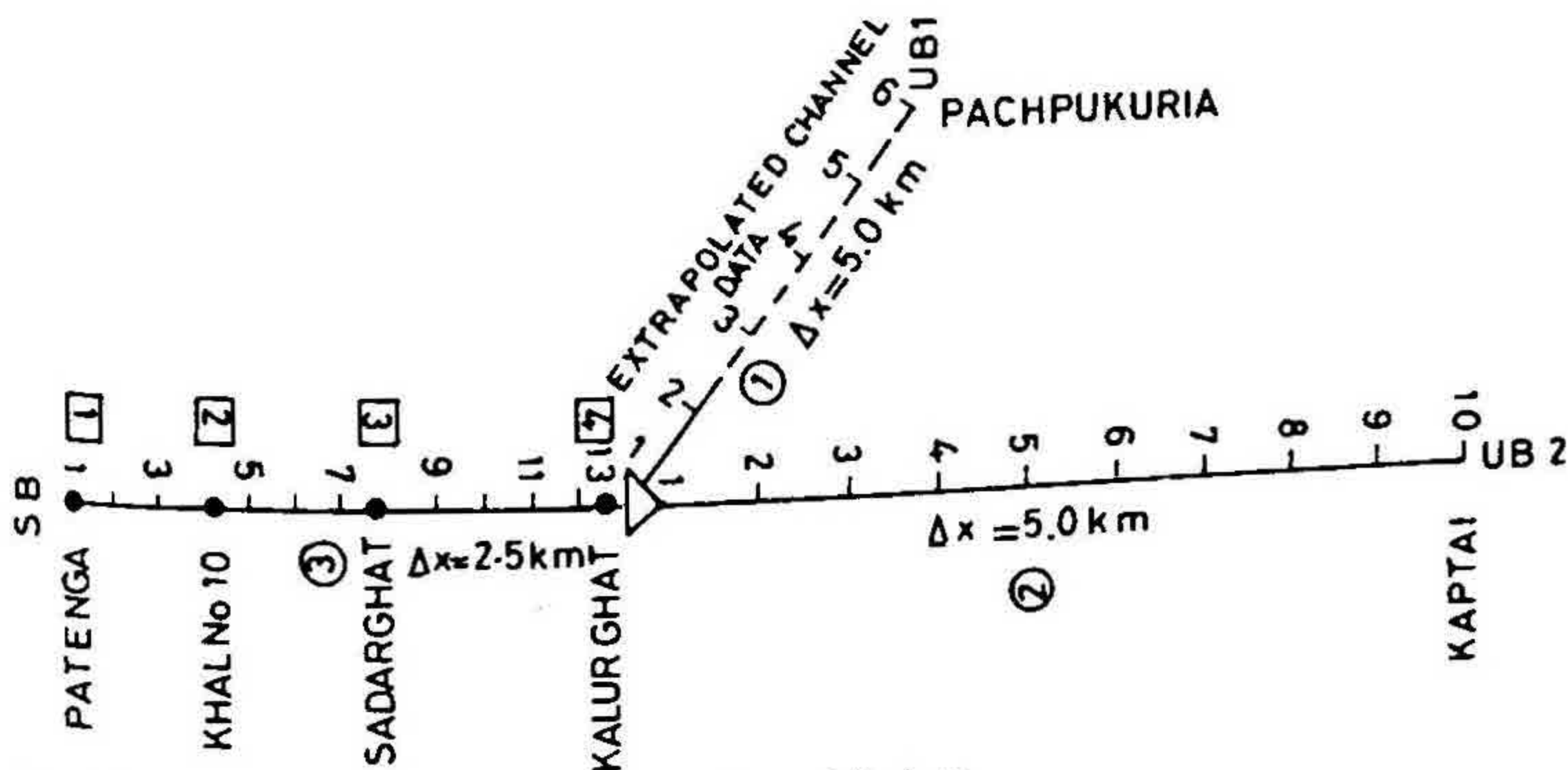


FIG. 2. Schematic representation of the Karnafuli river.

charts of the reach between Pachpukuria and Halda Bridge were not available. Hence the geometric properties of this reach were estimated by extrapolating the available sounding data of the Halda.

7. Calibration and validation of the model

7.1 Hydrodynamic submodel

The hydrodynamic model was calibrated⁹ by adjusting the Manning's-roughness coefficient to simulate the tidal stage at Khal No. 10, Sadarghat and Kalurghat using spring tide of range 5 m. For the calibrated values of $n = 0.027 \text{ m}^{-1/3} \text{ s}$ for the Karnafuli and $n = 0.04 \text{ m}^{-1/3} \text{ s}$ for the Halda, the model was validated by neap tide. At the upstream boundaries fluvial inflows were specified. The results of model calibration and validation are shown in fig. 3. The time step used in the application of the model was 900 seconds.

7.2 Salinity submodel

Sufficient data for detailed calibration and validation of the salinity model are not available. However, some data collected by the Netherlands Economic Institute (NEI)¹¹ and

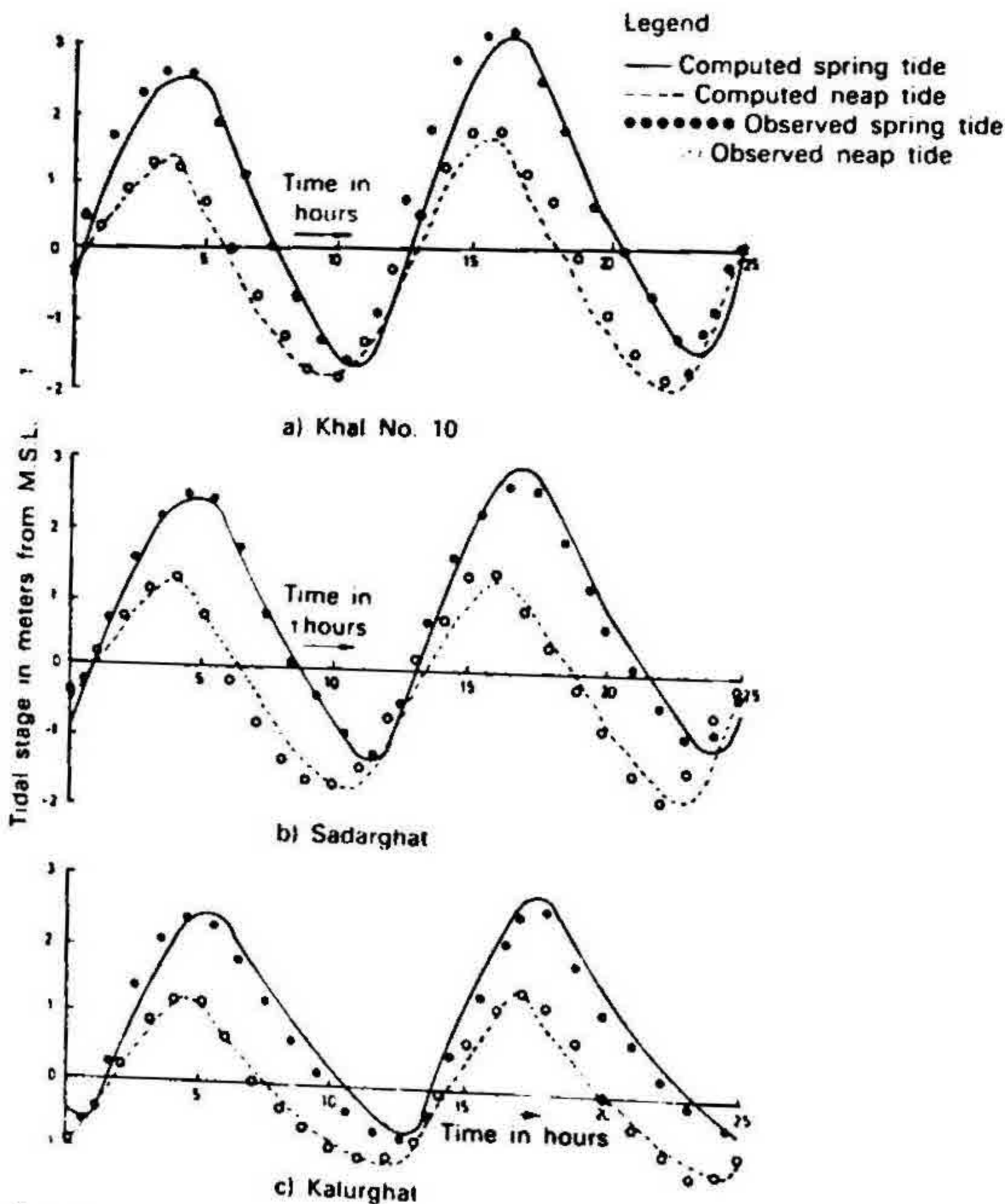


FIG. 3 Calibration and validation of the hydrodynamic model.

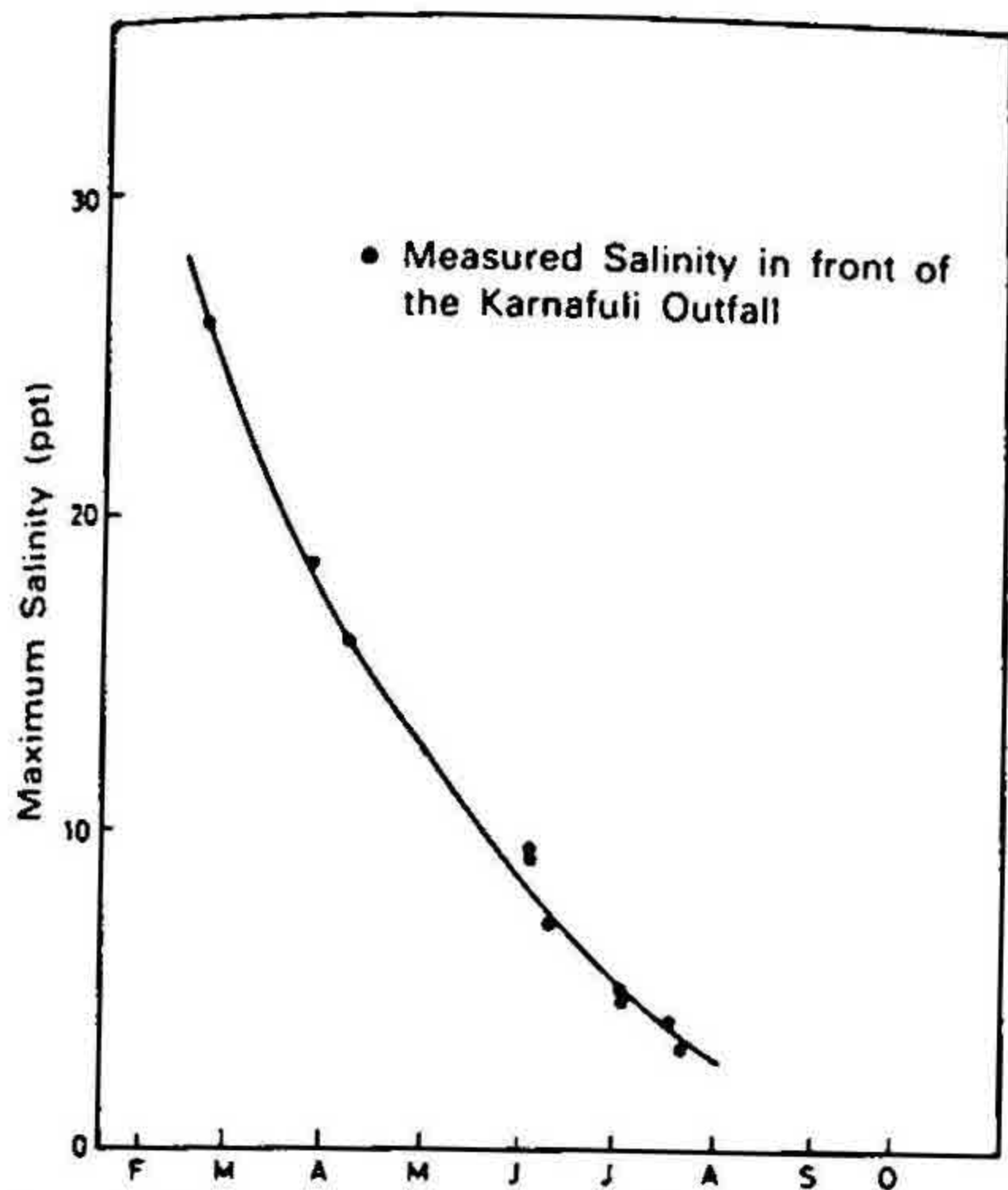


FIG. 4. Seasonal variation of salinity in the Bay of Bengal near Patenga.

the CPA¹² can be used for estimating the calibration coefficients in equation (4). Figure 4 taken from NEI shows the seasonal variation of salt concentration in the Bay of Bengal just the downstream of Patenga. NEI data also contains time variation of salinity over a tidal cycle at Patenga and information about salinity-intrusion length, which varied from 15 km during neap tide to 25 km during spring tide in April 1977.

To calibrate the model, it was run with spring tide on April 20, '77 with different values of K_1 . Since the effect⁶ of K_2 on salinity distribution is small a constant value of $K_2 = 250$ was assumed. Upstream inflows at Kaptai in the corresponding period was 117 cumecs. As information about the discharge at Pachpukuria was not available, its value was taken as 5 cumecs, which corresponds to dry-season mean value¹³. Figure 5a shows the longitudinal distribution of high-water slack (HWS) salinity in the Karnafuli river for different values of K_1 . The figure indicates that $K_1 = 50 \text{ m}^2/\text{s}$ represents the situation when the salinity-intrusion length is approximately 26 km. The model was then run for neap tide on April 21, '77 with calibrated values of K_1 . The water released from Kaptai was 300 cumecs. The discharge at Pachpukuria was kept unchanged. Figure 5 also shows the HWS salinity in the river for the neap tide. The salinity-intrusion length is about 14 km, which is close to the reported value. Recently, the CPA¹² collected HWS and low-water slack (LWS) salinity data along the length of the river over approximately three tidal cycles. With the calibrated values of calibration coefficients, the model was run for the tidal cycles. Figure 5b compares the computed HWS and LWS salinity with the corresponding field data.

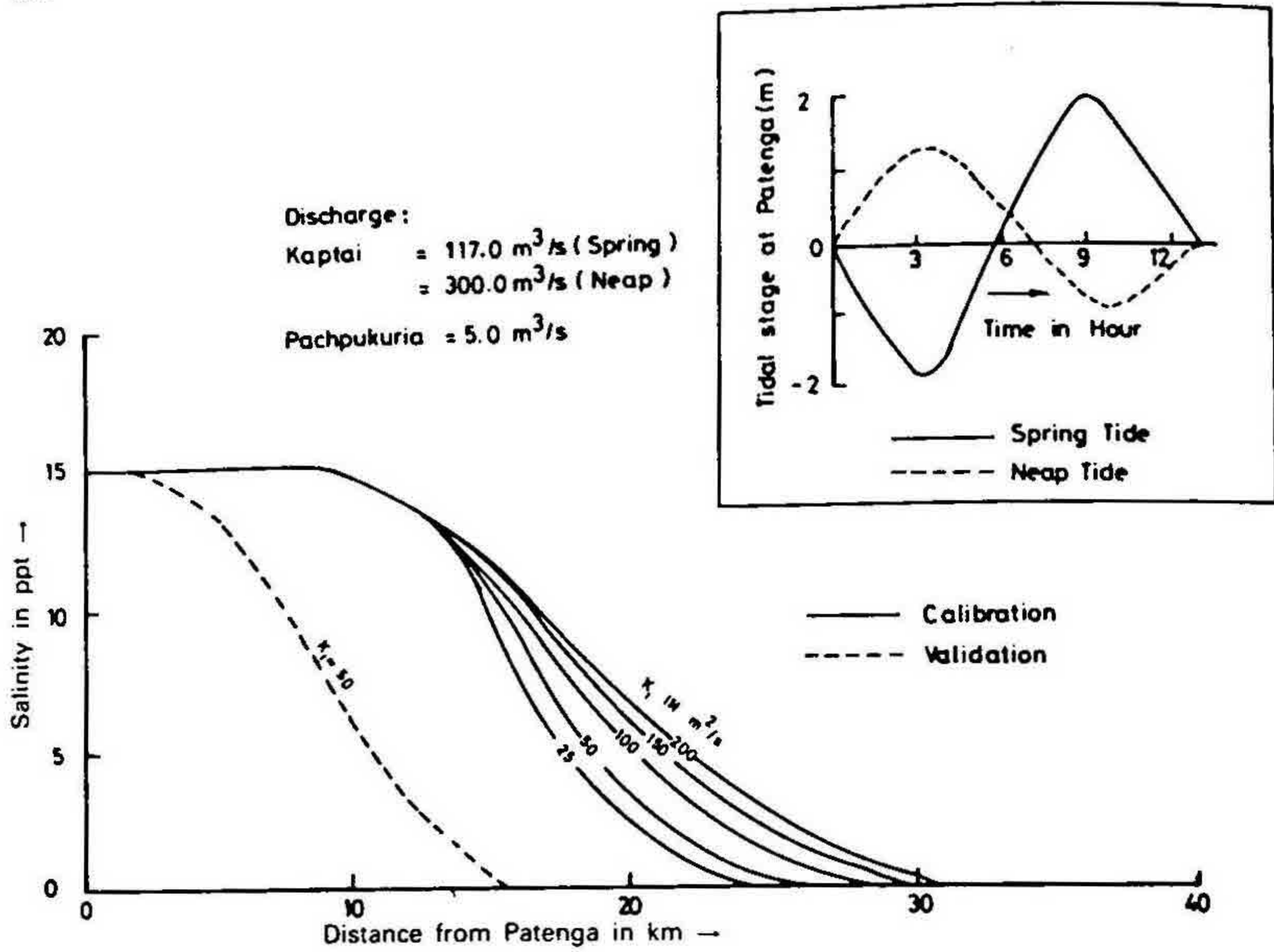


FIG. 5a. Calibration and validation of salinity model.

8. Results and discussion

8.1 Salt concentration of sea water at Patenga

Figure 4 indicates that the salt concentration of sea water at the outfall of the Karnafuli varies from 26 ppt in March to only 3 ppt in August. This reduction in salinity is caused

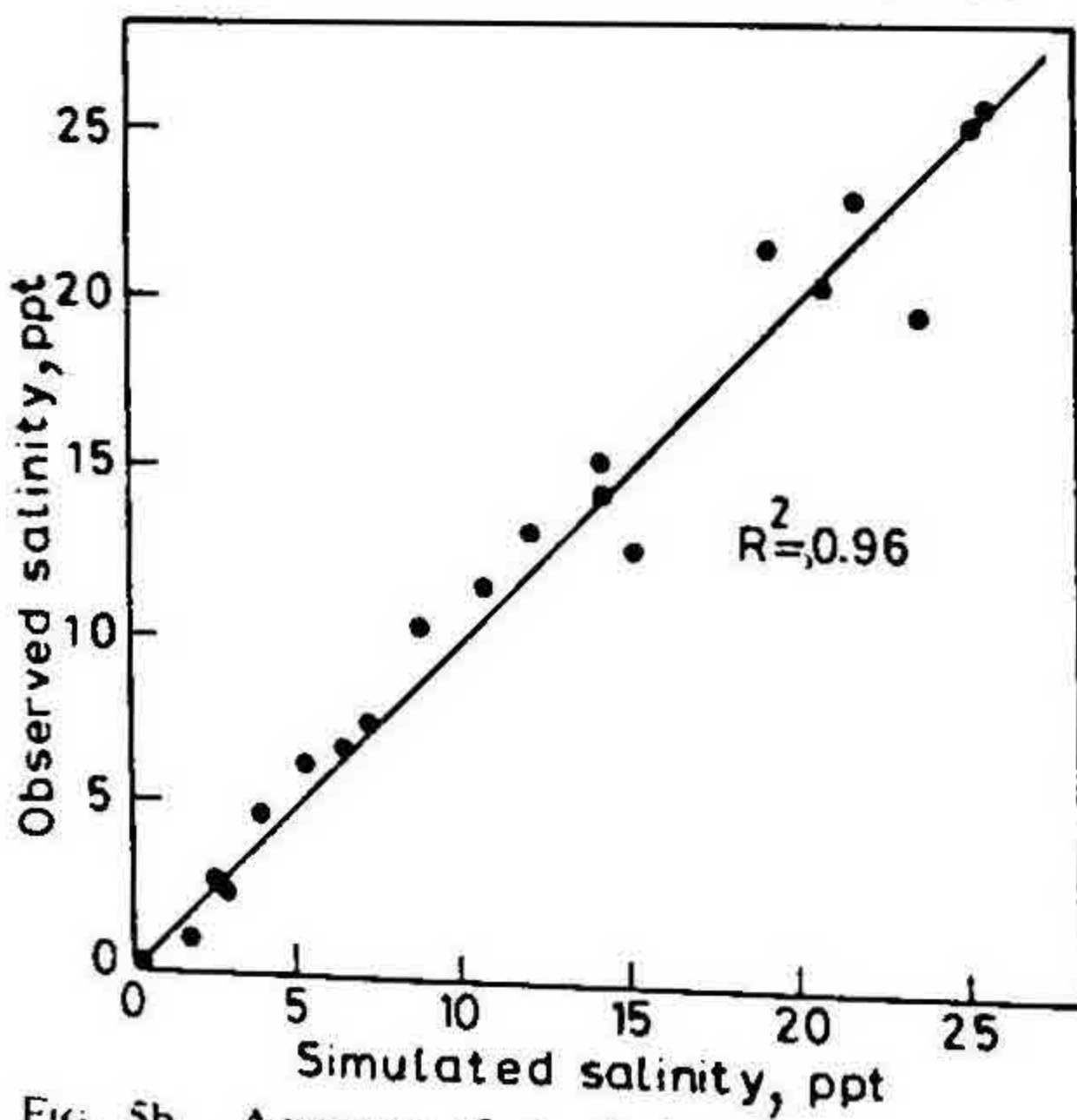


FIG. 5b. Accuracy of simulation.

by the combined influence of huge fresh-water discharge of the Ganges and the Meghna rivers in the northern part of the Bay of Bengal and the predominant south-western wind in the monsoon¹¹. During this period enormous amount of fresh water and favourable wind set up pushes the salinity front away from the coastal area. With the onset of dry season, the salinity front starts moving towards the coast. Consequently, salinity at the entrance of the Karnafuli shows a marked seasonal variation. In the wet season¹¹, saline water is frequently flushed out of Karnafuli at LWS.

8.2 Applicability of the model

The dispersion coefficient $E(x, t)$ expressed by equation (4) is applicable to well-mixed and partially mixed estuaries^{2,6}. In applying the model to the Karnafuli river, it is implicitly assumed that the vertical stratification of flow is negligible. In the absence of vertical-salinity data, the degree of stratification can be estimated by 'estuary number' defined⁶ as follows:

$$E_o = \frac{P_t F_t^2}{Q_f T} \quad (13)$$

where

P_t = tidal prism, defined as the volume of water entering the estuary in the flood tide.

F_t = densimetric Froude Number,

$$= \frac{u_o}{\sqrt{gh \frac{\Delta\rho}{\rho}}}$$

u_o = maximum flood velocity,

h = mean depth at estuary mouth,

ρ = density of water,

Q_f = fresh-water inflow, and

T = tidal period.

An estuary is stratified if E_o is relatively small. When E_o is high, saline water is mixed more uniformly by strong tidal action. During this study, the model was run with tidal range varying from 5 to 2 m. Upstream inflows varied from 10 to 500 cumecs. The computed tidal prism was found to vary from 63.81 to 192.36 million meter cubes. Flood velocity at Patenga varies from 0.92 to 1.26 m/s. From the analysis of geometric data, the mean depth of flow was estimated to be 11.5 m. In equation (13) $\Delta\rho$ represents the change in density of water over the whole length of river. Therefore, the ratio⁵ $\Delta\rho/\rho$ can be assumed to be around 0.026. Using appropriate values of other variables in equation (13), E_o was found to vary from 4.7 to 8.3. The analysis of a large number of estuaries by Thatcher and Harleman⁶ shows that E_o in general varies from 0.1 to 100. From the range of values of E_o in the Karnafuli river, it can safely be concluded that the Karnafuli is a well-mixed estuary. Consequently, the use of equation (13) to express dispersion coefficient is justified.

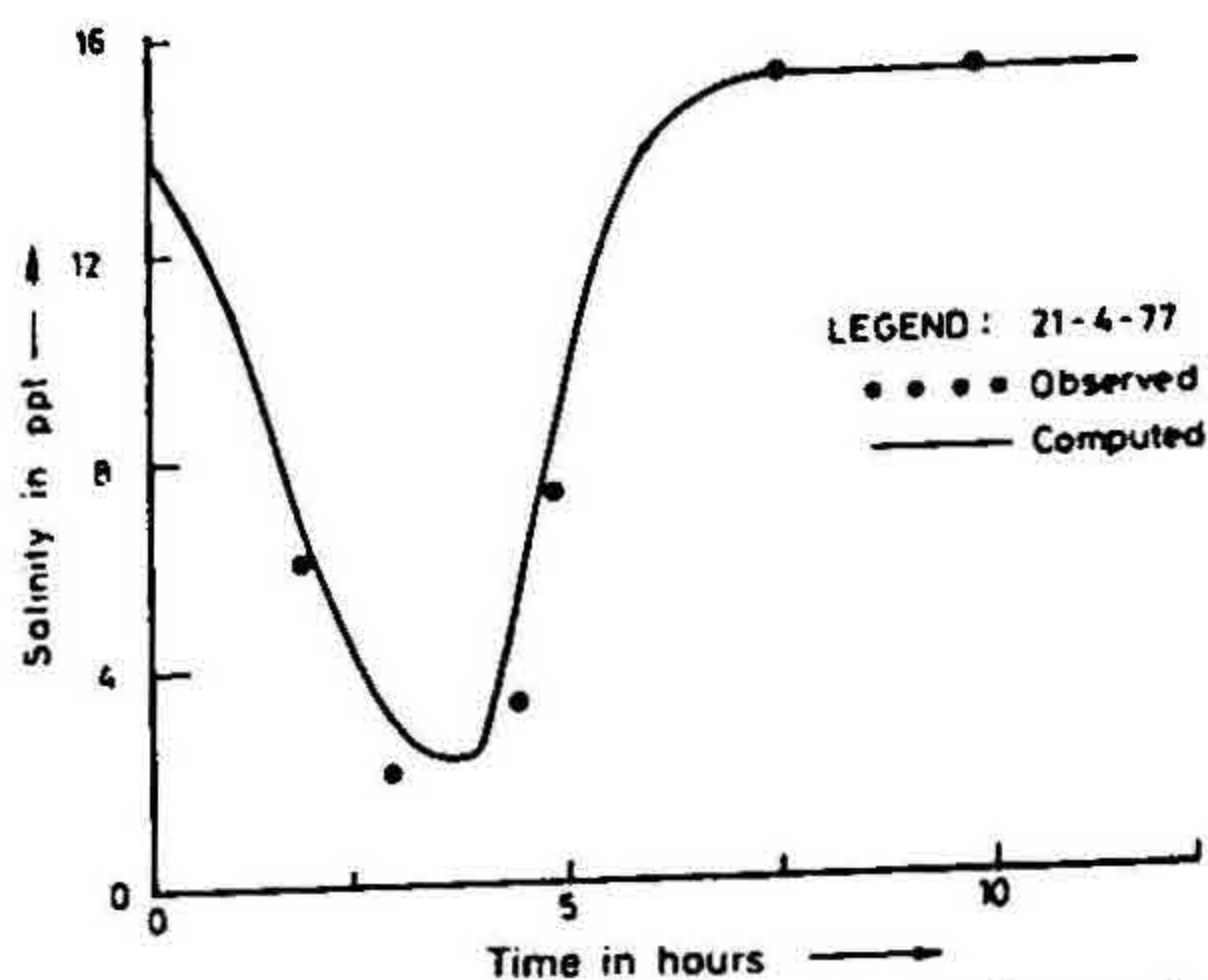


FIG. 6. Comparison of computed and observed salinity at Patenga.

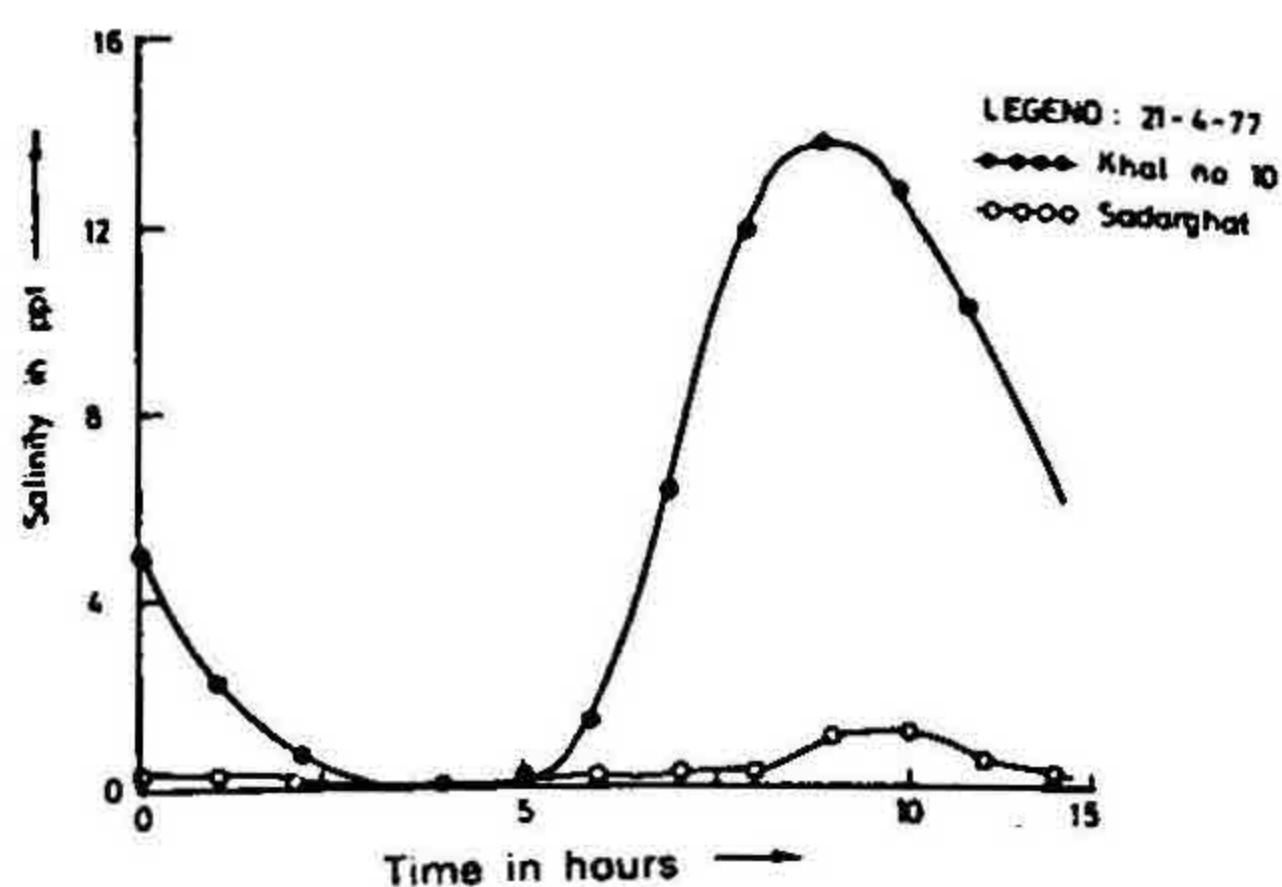


FIG. 7. Temporal variations of computed salinity.

8.3 Computation of boundary salinity at Patenga

The numerical model computes boundary salinity at Patenga from the salinity distribution in the river and the salt concentration of sea water. NEI data at Patenga, over a tidal cycle, provides an excellent opportunity to check the model formulation for sea face. Assuming that the period of linear interpolation of salinity from LWS value to sea salinity, when flow reversal occurs at the end of the ebb tide, is 0.20 of tidal cycle, fig. 6 compares the computed and observed salinity at Patenga. Considering the simplifying assumptions necessary⁶ in computing sea-face salinity, the model has simulated the variation of salinity at Patenga, over the tidal cycle, very well. The corresponding temporal variations of salinity at Khal No. 10 and Sadarghat are shown in fig. 7. Salinity at Kalurghat during this period was practically zero.

8.4 Calibration coefficients

The objective of model calibration and validation is to select proper values of K_1 and K_2 , which can not be directly determined from the field data. Sensitivity analysis⁶ of these coefficients indicates that salinity distribution is much more sensitive of K_1 . Adjustment of K_2 in calibration process is justified only when extensive field data are available for 'fine-tuning' of the model. The effects of varying K_1 on the computed longitudinal distribution of HWS salinity for given upstream inflow and tidal range are shown in fig. 5a. Increasing K_1 by eight times, salinity-intrusion length changes by 6.5 km or 26% of the reported salinity-intrusion length. Corresponding increase of K_2 hardly produces any change in the computed salinity. Thus it can be concluded that salinity intrusion in the Karnafuli is much more due to advection compared to dispersion, and dispersive transport is mainly due to longitudinal salinity gradient as represented by the first term in equation (4). To ascertain the quality of model calibration, it was used to simulate HWS and LWS salinity at three locations over three tidal periods. Figure 5b shows that the model has simulated the field data reasonably well. The coefficient of correlation R^2 , which gives a statistical measure of the performance of the model in terms of

'goodness of fit', was 0.96. Considering that the model was calibrated by locating the toe of salinity-intrusion length, the correlation coefficient is very high. Hence, for an estuary where convective transport plays major part in the transport of salt, a rough estimate of K_1 from available field data can give quite reasonable results for practical purposes.

An interesting point noted during the model calibration is that numerical instability occurs for K_1 values near $250 \text{ m}^2/\text{s}$ and the model becomes completely unstable for K_1 values greater than $325 \text{ m}^2/\text{s}$. For the given boundary conditions, increasing K_1 causes the model to transport more saline water. Finally a stage is reached when the river system can no longer transport the amount of saline water that the model numerically tries to transport. Consequently, numerical instabilities appear and the model becomes unstable.

8.5 Practical applications

As a practical application of the model, the effects of water released from the Kaptai dam during the dry season were studied. For a constant tidal range of 5 m at Patenga and S_0 equal to 25 ppt, fig. 8 shows the spatial variations of HWS and LWS salinity in the Karnafuli river as a function of upstream inflow of fresh water. The figure indicates a progressive increase of salinity-intrusion length due to the withdrawal of water. When the upstream inflow is less than 100 cumecs, salinity is found to penetrate upstream of the confluence of the Karnafuli-Halda river system, which is situated at a distance of 30 km from Patenga. If fresh-water inflow to the river system is around 10 cumecs, salinity reaches about 12 km upstream of the confluence. Even the toe of LWS salinity

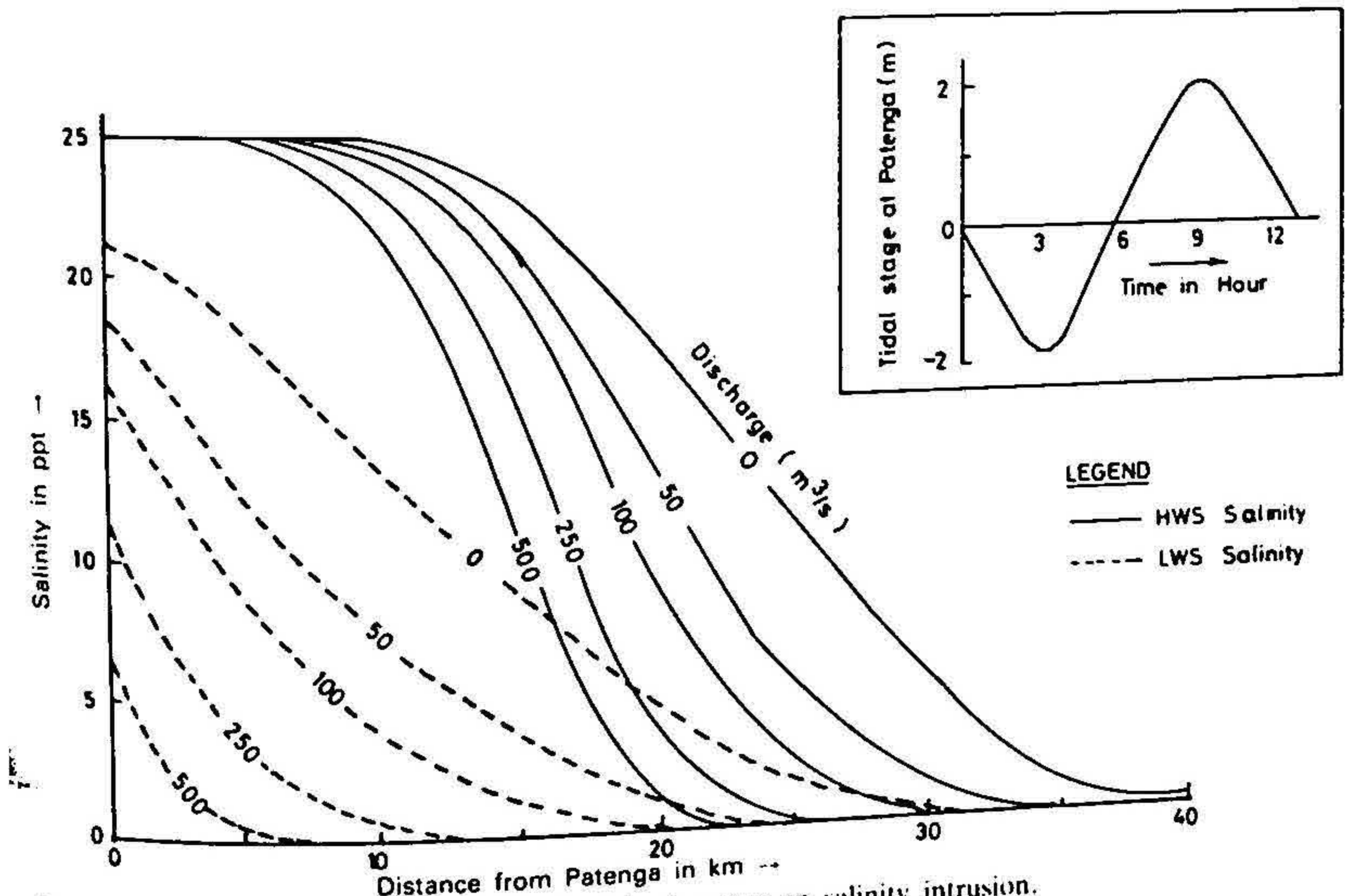


FIG. 8. Effects of upstream withdrawal of fresh water on salinity intrusion.

crosses the confluence. This is a situation which has not been observed after the completion of Kaptai dam¹¹ in 1962. However, in 1986 there was a severe drought in the Karnafuli river basin. Water level had fallen abnormally below the designed low-water level in the Kaptai lake and most of the power-generating units of the dam were shut down. Unfortunately, no record is available to indicate the extent of salinity intrusion, but it is likely that it had penetrated well upstream of the confluence as indicated by the model. The figure further indicates that completely undiluted saline water from the Bay of Bengal can penetrate about 12 km into the river.

Figure 9 shows the variation of salinity-intrusion length against combined upstream inflow as a function of tidal range at Patenga. When the net upstream fresh-water inflow is very small, salinity-intrusion length appears to be practically independent of tidal range at Patenga. The highest value of salinity-intrusion length is about 42 km. The situation changes rapidly as fresh-water inflow increases. When the inflow is 200 cumecs, salinity-intrusion length at 4.5 m tidal range is about 5.5 km greater than that at 2 m tidal range. An important information indicated by this figure is the efficiency of the additional fresh water in arresting salinity intrusion. The slope of the curves indicates that additional fresh water becomes increasingly less effective in diluting saline water. For example, when fresh-water inflow increases from 50 to 100 cumecs, salinity-intrusion length decreases by 6 km at 4.5 m tidal range. However, when the inflow increases from 100 to 200 cumecs, salinity-intrusion length decreases by only 4.5 km. At higher discharges the effectiveness decreases more rapidly. In dry season, fresh-water inflow from the Halda is negligible. Water released from the Kaptai dam is governed by the requirement of hydroelectric-power generation and the availability of water in the Kaptai lake. Figure 9 can be used as an approximate operating guide for the release of water from the dam, so

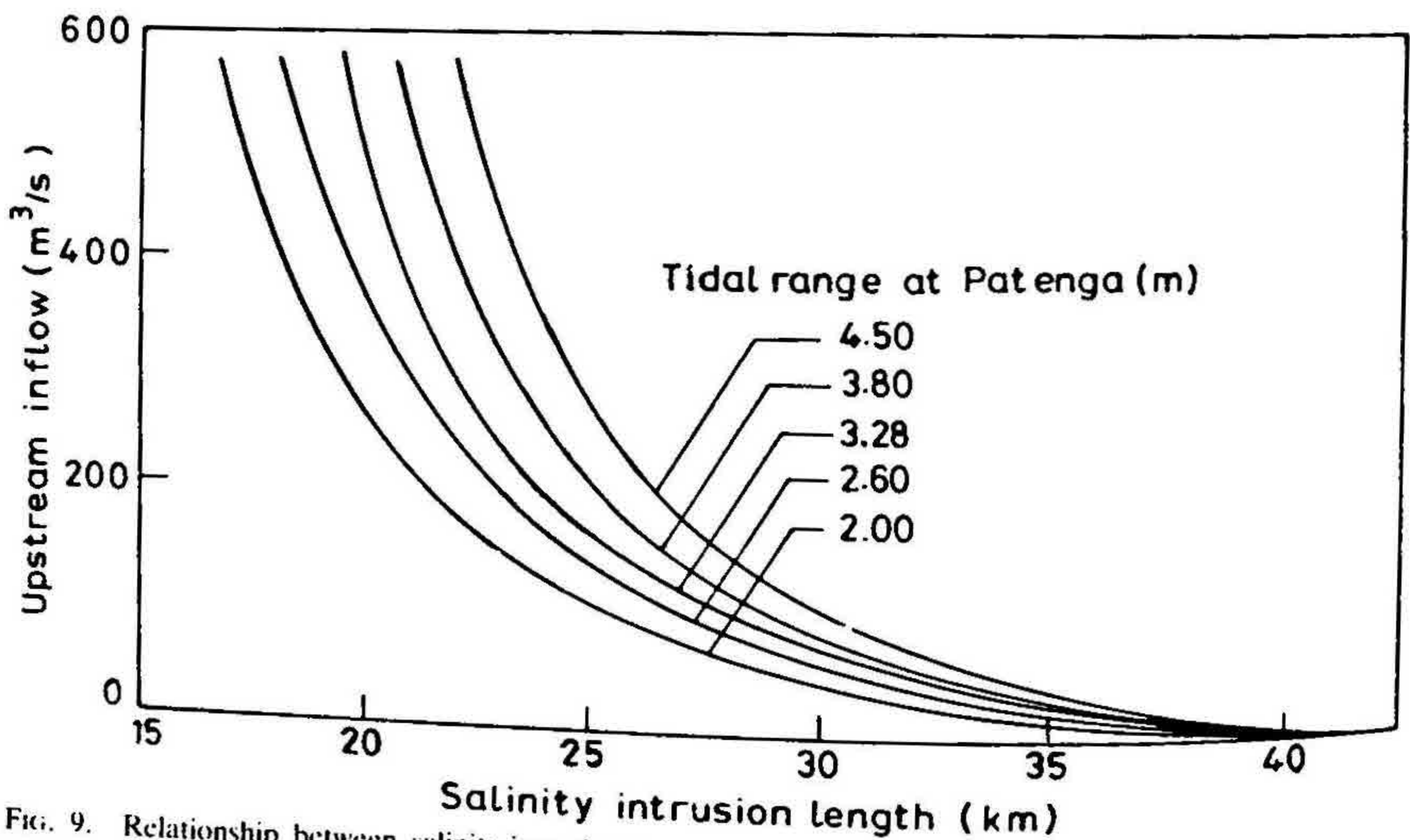


Fig. 9. Relationship between salinity-intrusion length, upstream inflow and tidal range.

that salinity in the lower reach of the Karnafuli can be arrested within certain acceptable limits.

9. Conclusions

The numerical model presented in this paper can compute spatial and temporal variation of salinity at discrete time and space intervals in the Karnafuli-Halda river system. Hydraulic information necessary for the determination of salinity distribution is obtained from a hydrodynamic model. The model was calibrated and validated by locating the toe of salinity front under two extremely different hydraulic conditions. The model calibration was further checked by simulating the HWS and LWS salinity over three tidal cycles. High coefficient of correlation indicates that the lack of sufficient field data for model calibration and validation should not limit the applicability of the model for most practical purposes. Sensitivity analysis of the calibration coefficients indicates that salinity intrusion in the Karnafuli river is mainly determined by convection of salt mass by the flowing water. The formulation of boundary condition at sea face appears to be consistent with the available field data. Graphical relationships between the salinity-intrusion length, the upstream fresh-water inflow and the tidal range at Patenga have been presented. These relationships can be used to estimate the approximate salinity-intrusion length under different hydraulic conditions. Therefore, it is expected that this model will be a useful engineering tool for long-term analysis and prediction of salinity intrusion in the Karnafuli river.

References

1. TRACOR *Estuarine modelling: An assessment*, Water Quality Office, Environmental Protection Agency, Corvallis, Oregon, USA, 1971.
2. DAILY, J. E. AND HARLEMAN, D. R. F. *Numerical model for the prediction of transient water quality in estuary network*, Rep. No. 158, Ralph M. Pearsons Laboratory, Dep. of Civil Engineering, MIT, Massachusetts, USA, 1972.
3. KHAN, L. A. AND ALAM, M. K. A one-dimensional numerical model of salinity intrusion of the Pussur River, *Bangladesh J. Wat. Resources Res.*, Dhaka, Bangladesh, 1985, 6(1).
4. CHOWDHURY, J. U. Prediction of saline water intrusion in the Meghna Delta. *Workshop on mathematical modelling in natural and social sciences*, Dhaka, Bangladesh, 1986.
5. McDOWELL, D. M. AND O'CONNOR, B. A. *Hydraulic behavior of estuaries*, MacMillan, 1977.
6. THATCHER, M. L. AND HARLEMAN, D. R. F. *A mathematical model for prediction of unsteady salinity intrusion in estuaries*, Rep. No. 144, Ralph M. Pearsons Laboratory, Dep. of Civil Engineering, MIT, Massachusetts, USA, 1972.
7. BERKHOFF, J. C. W. Transport of pollutants or heat in a system of channels, *Hydraulic research for water management, Proc. of Tech. Meeting No. 26*, Delft Hydraulics Laboratory, The Hague, 1973.

8. CUNGE, J. A.,
HOLLEY, F. M. AND
VERWEY, A. *Practical aspects of computational river hydraulics*, Pitman, 1980.
9. KHAN, L. A. A one-dimensional numerical model for the simulation of tides in the Karnafuli River, *J. Indian Wat. Resources Soc.*, Roorkee, India, 1986, 6(2).
10. STONE, H. L. AND
BRIAN, P. L. T. Numerical solution of convective transport problems, *J. A.I.Ch.E.*, 1963, 9.
11. *Chittagong Port entrance study*, Draft Final Rep., The Netherlands Economic Institute, Rotterdam, The Netherlands, 1977.
12. *Mathematical model study of the Karnafuli River*, Final Draft Rep., The Chittagong Port Authority, 1987.
13. *Surface water availability*, Vol. II, National Water Plan Project, Second Interim Rep., Master Plan Organization, Govt. of Bangladesh, 1984.